Dynamic analysis of a multi-column TLP floating offshore wind turbine with tendon failure scenarios

Dynamic Analysis of a Multi-column TLP Floating Offshore Wind Turbine with Tendon Failure Scenarios

Yajun Ren [a], Vengatesan Venugopal [a], Wei Shi [b, c] *

[a] Institute for Energy Systems, the University of Edinburgh, Edinburgh, EH9 3BF, UK

[b] DeepWater Engineering Research Centre, Dalian University of Technology, China

[c] State Key Laboratory of Coastal and Offshore Engineering, Dalian University of Technology, Dalian, China

* Correspondence: weishi@dlut.edu.cn (W. Shi)

Abstract

This paper presents the design and dynamic analysis of a multi-column tension leg platform floating offshore wind turbine (TLP FOWT) with broken tendons. The proposed concept is based on a conventional Tri-Floater platform configuration but is especially optimized for an intermediate water depth of 60 m. Tendons are simulated to be broken at a specific time of interest. The hydrodynamic parameters and motion responses of the TLP FOWT have been calculated using the hydrodynamic analysis software WAMIT and ANSYS/AQWA. These parameters are then used in the simulation of coupled responses of the FOWT by the National Renewable Energy Laboratory's analysis suite of tool, FAST. The tendon failure has been investigated to examine the system performance under the accidental limit states (ALS) described in the design code DNV-RP-0286.

A series of dynamic analysis under operational and extreme environmental conditions (with 12 different load cases) are carried out with the combination of wind and waves. The results demonstrate that the turbine is able to remain highly stable during the 3-hour simulations conducted. The platform's response amplitude operators (RAOs) evaluated show

good stability in heave and pitch. The tendon failures affected the FOWT's heave, pitch and roll motions, hence its natural frequencies, and the tension in the non-broken tendons. The average tensile force in the line adjacent to the broken line is found to be doubled, while the safety factors as specified in DNV-OS-E301 are remained within the recommended value. This paper provides further insights into the hydrodynamics of the multi-column TLP FOWT, with the aim to provide new information to the offshore wind research community.

Keywords: Floating offshore wind turbine; TLP; tendon failure; accidental limit state; dynamic response analysis

1. Introduction

Offshore wind energy is turning to a mainstream energy source and deployment of offshore wind turbines have accelerated during the past decade. Ten percent of global new wind power installation in 2019 was contributed by offshore wind sector, and the share is expected to be more than 20% by 2025 (GWEC, 2020). Wind energy availability in the ocean at water depths larger than 50 m has the advantages of consistent higher energy density, where the floating offshore wind turbine (FOWT) is considered as a more cost-effective alternative compared to the fixed-bottom wind turbines such as monopiles or jacket type designs. As of 2019, a total of 65.7 MW floating wind has been installed worldwide (GWEC, 2020; Zeng et al., 2021), including the WindFloat Atlantic, a 25-MW floating offshore wind farm installed 20 km offshore Viana do Castelo, Portugal (EDP, 2021); a 2-MW Ideol Damping Pool FOWT of Floatgen project at France (Ideol, 2021); the Hywind Scotland 30-MW windfarm installed 25 km away from the coastline of Peterhead (Equinor, 2021).

The support platform of floating offshore wind turbines is typically classified into four main categories based on how the concepts achieve static stability (Matha, 2009) and these are barge, spar, semi-submersible and tension leg platform (TLP). Among the above concepts, TLP is seen as one of the most stable platform concepts and have less impact on the wind turbine dynamics (Crozier, 2011). For typical configuration of floating platforms, such as semi-submersible, spar and barge, the motions in both translational and rotational modes are significant due to the compliant nature of the catenary mooring system. Whereas, for TLPs, the taut tendons restrict the motion, the structure has lower heave and pitch responses in much of the operating frequencies, as well as small mean surge and sway displacements during operation (Vijay et al., 2018). In addition, the natural frequencies of the platform fall out of the range of high-density energy area of the waves, which effectively reduce the risk of resonance.

Several studies have been carried out on the design and analysis of TLP-type FOWTs. A preliminary design of a TLP platform coupled with a NREL 5-MW wind turbine, consisting of a column and four spokes for a water depth of 200 m, was conducted by Withee (2004), and, the model was then optimized and the dynamic performance was further analyzed by Matha (2009) using the fully coupled simulation tool FAST (Jason M. Jonkman & Jr., 2005). The model was scaled up by Crozier (2011) for supporting a 10-MW wind turbine developed by NOWITECH, which demonstrated the feasibility of TLP to support the large size turbine. A tension leg buoy was designed by Myhr (2016) who used 3DFloat, an aero-hydro-servo-elastic analysis software package developed at Institute for Energy Technology (IFE), Norway. The technical and economic analysis were carried out, indicating that the TLB type FOWT has potential to compete with onshore wind turbines in Japan and Australia and can be seen as one of the options in European market. Based on the conventional single column configuration, several multi-column concepts are proposed, such as WindStar (Y. Zhao et al., 2012) and the four pontoon submersible floating platform (Ding et al., 2016). These studies addressed the advantages of multi-column TLP, such as its better stability and easy

installation since wet tow can be achieved by proper ballasting and de-ballasting for the self-stable configuration. A three-column semi-submersible FOWT named Tri-Floater was initially designed by GustoMSC (2021) for commercial purpose. The concept was investigated by Lefebvre and Collu (2012) and a preliminary modification was made by replacing the catenary mooring system by a taut mooring system to improve the hydrodynamic performance of the platform. The study shows that the combination of the tri-floater conceptual platform and the taut mooring system can be seen as the most promising configuration.

The present study aims to optimize and investigate the above stated Tri-Floater platform which is featured by a taut mooring system, based on the recommendation of the design and analysis standards DNVGL-ST-0119, DNVGL-RP-0286 and DNVGL-OS-E301(DNVGL, 2015, 2019, 2018). The redesign of the platform was especially aimed for a water depth of 60 m, which is the shallowest among the recommended TLP FOWT installation depth. The previous TLP designs mainly focused on the water depth more than 150 m, and this poses a huge challenge to carry out construction at such water depth due to the technical and economic limitations (Zhao et al., 2021). In addition, several countries (e.g. China and South Asian countries) with great ambition of developing floating offshore wind technologies, have deployment water depth around 60 m, will benefit from the concept proposed here. The multi-column platform provides sufficient buoyancy and high rotational moment of inertia, which ensure the good stability during operational phase with the application of well-designed taut mooring system. The self-stability is possible by proper ballasting during towing phase, wet tow is therefore achieved to simplify the installation and reduce cost.

The specific content included in the DNV standards for TLP-type FOWT particularly points out the requirement of mooring failure analysis as an ultimate state considering the crucial role of mooring system for the structural stability. The damage of one tendon may cause the sudden increase of tension in the remaining tendons, leading to progressive failure

of the mooring system and even the whole structure of the FOWT. Without the robust design including the mooring failure analysis, the consequences can be serious and costly, related to power loss, damage to environment and loss of the facilities, etc. Although no accidents have been reported yet in the FOWT industry as the number of commercial scale installations were small, the mooring line failure cannot be ruled out for the future deployments, because there were cases reported even in the oil and gas industry with more mature technologies in comparison to FOWT.

In the oil and gas industry, serious damages to the floating drilling units and production platforms in the Gulf of Mexico by hurricanes Katrina and Rita have been reported in Cruz and Krausmann (2008); nineteen MODUs have lost their moorings and became adrift during the storm, and, the drifting platforms caused 100 pipelines to be damaged. The other representative case happened on 29 May 2014, when 6 tendons of a Chevron's major drilling project in the US GOM failed and led to subsequent damage to three additional tendons in the following days. The accident directly resulted in the delay of the construction progress for four years (Whitfield, 2019). The mooring failure analysis on conventional O&G TLPs have been widely studied (Mansour et al., 2013; Qi et al., 2019; Yang & Kim, 2010; Yang et al., 2009). The above literatures demonstrate that the damage of tendon can affect the responses of the floating platforms, especially heave and pitch motions, as well as the force in the remaining tendons.

With reference to FOWTs, Bae et al. (2017) investigated the performance change of a semi-submersible FOWT after one mooring line failed. The results showed that the platform was subject to a large drift along the wind and wave incident direction. The mooring failure effect on the transient response of a spar-type FOWT was studied by Liu et al. (2018). Similar to the semi-submersible platform, a significant drift of the platform was observed, which could cause a risk of collision with the neighbouring turbine in the wind farm.

For TLPs, the taut station-keeping system results in different characteristics of the platform response in comparison to the catenary-moored system, such as semisubmersible and Spar FOWTs. In addition, the mooring system plays a more important role in maintaining the stability of the structure than the self-stabilized platform. Due to the combined effect of wind, waves and the operation of wind turbine, the responses of TLP FOWT after tendon failure can be more complicated, however, the literature on this particular type of FOWT technology appears scarce. Recently Wu et al. (2021) studied the transient response of the WindStar TLP system with one tendon failure. They reported several useful outcomes including the higher transient responses of the FOWT under operational conditions than the extreme condition corresponding to 50-years return period. However, the wind-wave misalignment was not accounted in the study, which is important to the responses of TLP FOWTs. In addition, only one tendon breakage was considered in the paper. Therefore, the present research was conducted to fill this gap. The coupled time-domain aero-hydro-servo-elastic-mooring simulation tool, FAST was employed with proper modification of the source code in the mooring module, MAP to achieve the tendon failure at the appointed time.

To conclude, a tension leg Tri-Floater platform with a NREL 5-MW wind turbine is redesigned for the present work which is suitable for a water depth of 60 m. The dynamic responses of the FOWT under the combined wind and wave conditions were analysed. The effects of tendon failure were especially addressed to examine the safety of the structure under the damaged condition. The novelties of the present paper are summarized as follows. Firstly, an innovative multi-column floating platform with a taut station-keeping system was redesigned based on the tri-floater platform. In addition, a water depth of 60 m was considered, which distinguishes the new designed FOWT from the conventional prototypes that are only applied for the deep ocean. This work shows the possibility of installing TLP FOWT at such a moderate water depth as an alternative for countries and areas longing for

developing FOWT without deep-water environment. For structure at intermediate water depth, the wave loading is more predominate and the performance under tendon failure scenario can be much different than that in deep water. Therefore, it is important to conduct the failure analysis for the present model. Additionally, a comprehensive tendon failure analysis is undertaken with consideration of wind-wave misalignment and different tendon to be broken, which was hardly seen in the previous studies.

The structure of the paper is given as follows. In Section 2, the design basis, background and objectives, the dimensions of the floating platform and the wind turbine, the theoretical principles of the simulation are described. In Section 3, the hydrodynamic characteristics, the natural frequencies and the response amplitude operators (RAOs) are evaluated. In Section 4, the environmental conditions of the load cases, the tendon failure scenarios and the dynamic responses of the FOWT under those conditions are investigated and discussed. The main findings of the present study are summarized in Section 5.

2. Design and modelling

2.1 Design basis

The floating platform is modified based on the concept firstly raised by GustoMSC as a three-column semi-submersible structure using catenary mooring system with a design water depth of 100 m (GustoMSC, 2021). Although a series of modifications were made for approaching to the industrialization, the initial concept were investigated in the study carried out by Lefebvre and Collu (2012), and identified as the most suitable concept of platform to support the NREL 5-MW offshore wind turbine at Dogger Bank. This site is located just over 130 km off the North East coast of England and considered as one of the most important targeted sites for developing offshore wind farm by the UK government. Rather than the catenary mooring system that have been widely used for semi-submersible platform, a set of

taut mooring system was selected for station keeping in the present study following the results presented by Lefebvre and Collu (2012). The taut system can significantly improve the stability of the platform and therefore reduce the impact of the platform motion on the turbine system. In addition, the combined semi-submersible platform and taut mooring system can effectively reduce the difficulty of transportation and installation, as the platform can be ballasted during towing with good stability and de-ballasted after the mooring system is installed. A preliminary design of the full FOWT structure including the platform and the mooring system was proposed considering the strength, static stability, and hydrodynamic characteristics of the system with the relevant environmental condition and site specifications applied.

In the present study, the platform is adapted based on the design standard DNVGL-ST-0119, DNVGL-RP-0286 and DNVGL-OS-E301(DNV, 2015; DNVGL, 2015, 2019, 2018) mainly aiming to meet the following requirement:

1. The natural period of the platform should fall into the range of 15-60 s, 1-2 s, 2-5 s and 8-20 s in surge, heave, pitch and yaw direction respectively;

2. The maximum tension force should not exceed the minimum breaking load (MBL) of the tendon and the safety factors shall be remained;

3. The tendon should not be slack in the Ultimate Limit State (ULS) and Accidental Limit State (ALS); and

4. The structure stability can be sustained with the partially failure of tendons.

To modify the platform from a catenary-moored system to a taut-moored system, the first objective is to determine the total pretension of the mooring system by adjusting the relationship between the platform displacement volume, i.e. the buoyancy, and the mass. In the present design, the draft of the platform was increased from 13.5 m to 16.5 m for higher buoyancy and therefore larger pretension of the mooring system. A 6-line configuration with 2 lines for each column was identified as the most technical and economic feasible option for

station keeping. The key properties of the mooring system, such as materials, axial stiffness, diameter and the location of fairleads and anchors are determined accordingly. Furthermore, the other properties, including the distance between columns, diameter of the heave plates, ballast water height, configuration of the beams and bracings etc. were also modified and optimized to ensure the FOWT to follow the design standards stated above. The detailed properties of the redesigned platform are described in the following section.

2.2 Model description

The FOWT structure consists of a NREL 5-MW offshore wind turbine, a floating platform and three pairs of taut mooring lines as illustrated in Fig.1. The properties and the configuration of the structure are described in this section.

Fig. 1. Schematic layout of the TLP wind turbine

The NREL Offshore 5-MW baseline wind turbine is utilized in the present study. The baseline model has been widely used throughout the world in the research of floating offshore wind energy technologies, such as J. Jonkman (2010) and Bae et al. (2017). The key specifications of the turbine are summarized in Table 1.

Table 1. Specifications of NREL 5-MW Baseline Wind Turbine

Parameter	**Value**
Rating	5 MW
Rotor Orientation, Configuration	Upwind, 3 Blades
Control	Variable Speed, Collective Pitch
Drivetrain	High Speed, Multiple-Stage Gearbox
Rotor, Hub Diameter	126 m, 3 m
Hub Height	90 m
Cut-In, Rated, Cut-Out Wind Speed	3 m/s, 11.4 m/s, 25 m/s
Cut-In, Rated Rotor Speed	6.9 rpm, 12.1 rpm
Rated Tip Speed	80 m/s
Overhang, Shaft Tilt, Precone	5 m, 5°, 2.5°
Rotor Mass	110,000 kg
Nacelle Mass	240,000 kg
Tower Mass	347,460 kg
Coordinate Location of Overall CM	(-0.2 m, 0.0 m, 64.0 m)

As illustrated in Fig. 2, the main body of the platform consists of (1) three cylindrical columns of 10 m diameter and 24.5 m height, (2) the heave plates with diameter of 18 m and height of 1 m attached at the bottom of the column (3) a centre column placed at the middle of the platform, and (4) the connecting beams and braces. The turbine is connected with the platform via the centre column, whose diameter is the same as the tower base, raising the

tower base up to the level of 10 m above the mean sea level. The distance from the centreline of the tower to the side column is 35 m. The platform will be installed in the water with the draft of 16.5 m. One column is placed upwards to the incident waves and the rest are in the leeward direction while the wind and waves are illustrated in the top view of the platform (Fig. 3). The coordination system is noted in red in the figure. The main dimensions and properties of the platform are illustrated and summarized in Figs. 3-4 and Table 2.

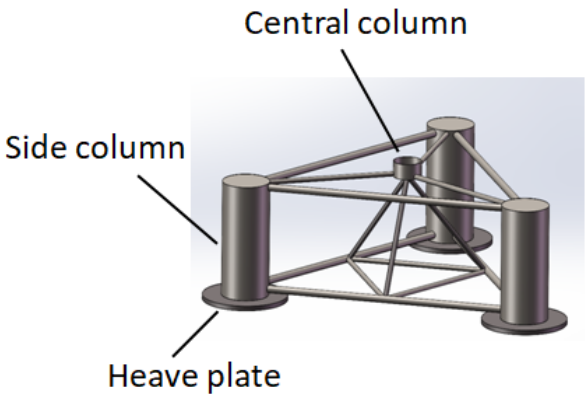

Fig. 2. 3D sketch of the floating platform

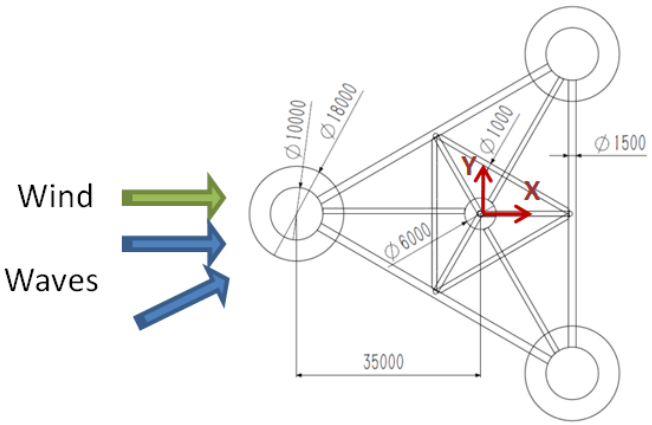

Fig. 3. Top view of the floating platform

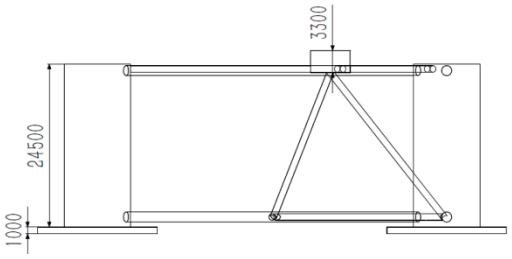

Fig. 4. Side view of the floating platform

Table 2. Properties of the TLP floating platform

Parameter	**Value**
Side column radius	5 m
Side column height	24.5 m
Centre column radius	3 m
Centre column height	3.3 m
Distance between tower and side column centrelines	35 m
Heave plate radius	9 m
Heave plate height	1 m
Platform mass	1890 ton
Water depth	100 m
Design draft	16.5 m
Displacement	4896 m^3
Vertical centre of mass (CM) below MSL	8.61 m
Moment of inertia in pitch/roll about the CM	1.21×10^9 kgm^2
Moment of inertia in yaw about the CM	2.209×10^8 kgm^2

A synthetic fiber rope is selected for station keeping considering to its light weight, high elasticity and minimum breaking load (Anchor, 2021). The taut mooring ropes are attached at the bottom centre of the heave plate, with a pair of lines for each column. Ropes are numbered

in a clockwise direction from the pair connecting with the upwind column (as illustrated in Fig.1). The properties of the mooring system are summarized in Table 3.

Table 3. Mooring system properties

Parameter	**Value**
Diameter	245 mm
Unstretched length	83.315 m
Number	6
Axial stiffness	4.99×10^8 N
Mass density in air	37.9 kg/m
Minimum breaking load	20307 kN
Total pretension	28500 kN

2.3 Introduction to numerical simulation tool

The numerical model of the floating offshore wind turbine was built using the fully coupled aero-hydro-servo-elastic-mooring analysis tool, FAST. The program integrates the environmental conditions (incident wind, waves and sea currents), wind turbine control system, structure dynamics and mooring dynamics together and simulates the performance (J. M. Jonkman, 2009).

The wind turbine structure consists of rotor-nacelle assembly (RNA), tower and support platform. The support platform is modelled as a rigid body with six degree of freedom (i.e., surge, sway, heave, roll, pitch and yaw), while the coupling between the motions of the platform and the RNA, as well as the tower are obtained by introducing the 22 degree of freedoms (DOFs) into the system's equation of motion. The general form of the coupled motion of the structure is presented as:

$$M_{ij}(q,u,t)\ddot{q}_j = f_i(q,\dot{q},u,t) \quad (1)$$

where, M_{ij} is the (i,j) component of the inertia mass matrix. The factors that affect M_{ij} are the set of system DOFs (q), control inputs (u) and time (t); $\ddot{q}_j$ represents the second time derivative of DOF j. The right-hand side of the Equation (1) indicates that the forcing function,

f_i nonlinearly depends on DOFs, q, and their first-time derivatives $\dot{q}$, control inputs, u and time t.

In addition to the complex body motions of the platform, the factor that distinguishes the FOWTs from the conventional fixed bottom wind turbines is the calculation of the forces on the support platform, which is implemented by Equation (2) in FAST:

$$F_i^{Platform} = -A_{ij}\ddot{q}_j + F_i^{Hydro} + F_i^{Lines} \quad (2)$$

where, A_{ij} is impulsive hydro dynamic-added-mass matrix of (i, j), F_i^{Hydro} and F_i^{Lines} are i_{th} components of the applied hydrodynamic loads and the mooring-lines imposed loads on the support platform respectively, which are included in the forcing function f_i in equation (1) (J. M. Jonkman, 2009).

The hydrodynamic loads on the FOWT can be calculated based on potential-flow theory and Morison's Equation. In the present study, a hybrid model with the consideration of both the above was created. To be specific, the potential-flow theory was used for the calculation of the hydrodynamic coefficients (hydrostatic restoring matrix, hydrodynamic added mass matrix and damping matrix) of the cylindrical columns and the heave plates. The relevant calculation was carried out by using the hydrodynamic analyses software WAMIT (WAMIT, 2019) and ANSYS/AQWA (ANSYS, 2017). For WAMIT, the finite element mesh was generated by the pre-processing software MultiSurf (refer to Figure 5), where the panel size is determined internally by assigning NU and NV (panel number in the two directions) on each patch. In this case, it is not generally possible to determine the exact size of the panels. However, the total number of panels used for the WAMIT analysis was 4800. When the mesh was generated in AQWA, a mesh size of 1 m was determined, and the total panels were 12903. Although a panel optimization study was not carried out, the fact that both WAMIT and AQWA produced the same results (see Section 3, Figure 6) indicate that the panel sizes used have not affected the results. These two software tools were used for the purpose of a code-to-code comparison and also to demonstrate the reliability of the results from the

hydrodynamic models. However, for further work, the results from WAMIT were only used as the output from WAMIT can be directly interfaced with FAST. The results obtained by WAMIT, was fed into the HydroDyn module of the FAST suite to obtain the hydrostatic restoring, wave radiation, and diffraction forces in time domain.

It is to be noted that the hydrodynamic analysis carried out by WAMIT, which was based on potential-flow theory, is applicable to structures that are large relative to a typical wavelength. For slender cylindrical structures (such as beams and braces as in Fig. 1), where the effects of diffraction and radiation damping are negligible and flow separation may occur, Morison's equation is normally considered to account for wave loading from incident-wave-induced excitation. Therefore, the beams and bracings were included in the input to the HydroDyn and simulations produced. The values of inertia and drag coefficients chosen for the Morison force calculation were 1.6 and 0.65 respectively.

The Mooring Analysis Program (MAP) was used in parallel with HydroDyn to model the forces on the mooring system, including elasticity, weight and geometric nonlinearities, based on a multi-segmented, quasi-static (MSQS) theory (Masciola et al., 2013). Once the mooring properties, material definitions, connections between lines and node properties are input, the simulator can calculate the mooring forces and integrate to ElastoDyn in time. To achieve the simulation of mooring failure condition, the interface of FAST to MAP program is adopted so that the interaction between the platform and the tether can be eliminated at the appointed fairlead and at a specific time of interest.

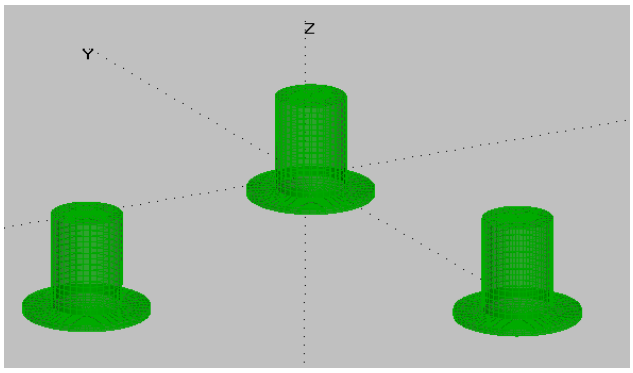

Fig. 5. Platform discretization with flat panels

3. Model verification

3.1 Hydrodynamic analysis

The non-dimensional added mass and damping coefficients calculated using WAMIT and AQWA are presented in Fig.6. The results show good agreement between the two software tools, demonstrating the reliability of the hydrodynamic models. The damping coefficient in heave at low frequency (lower than 1 rad/s) indicates that the presence of damping plate can effectively restrain the heave response of the structure. The non-dimensional wave excitation forces in surge, heave and pitch output from WAMIT are presented in Fig.7.

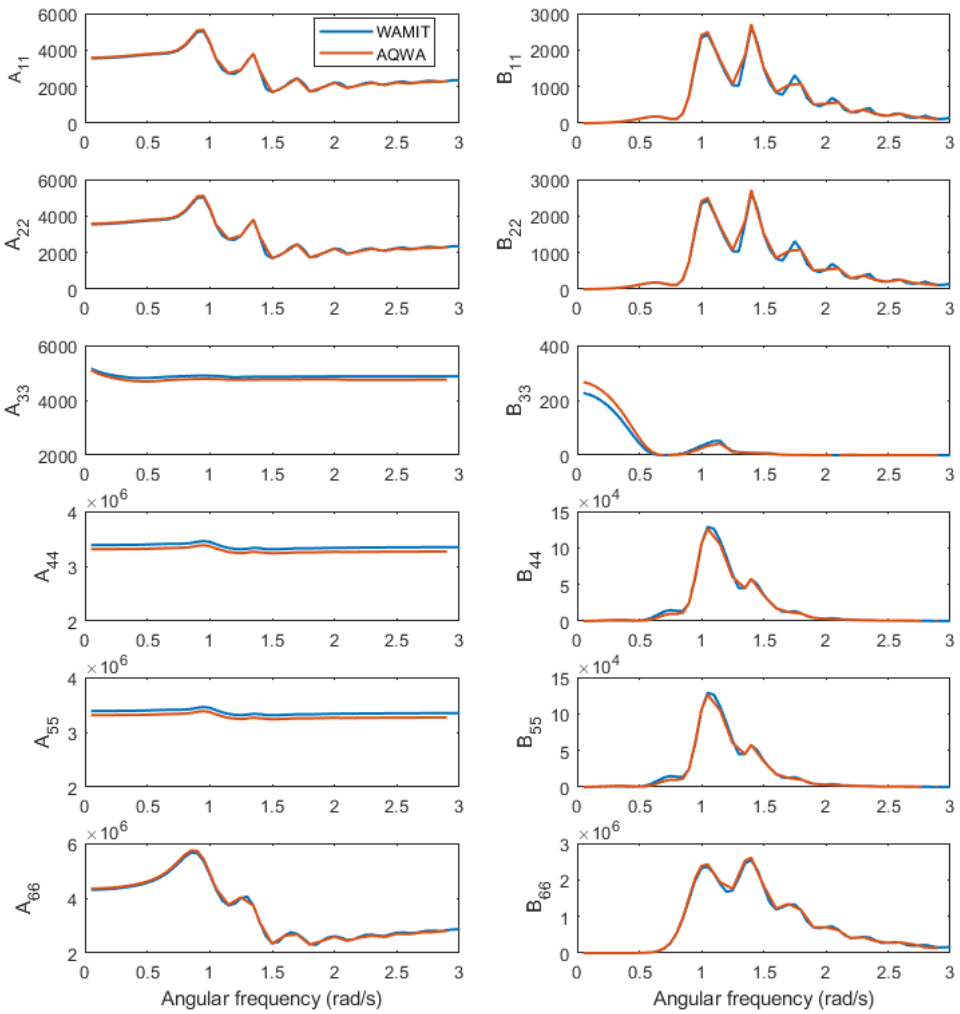

Fig. 6. Non-dimensional added mass and damping matrix coefficients of the platform calculated by WAMIT and AQWA

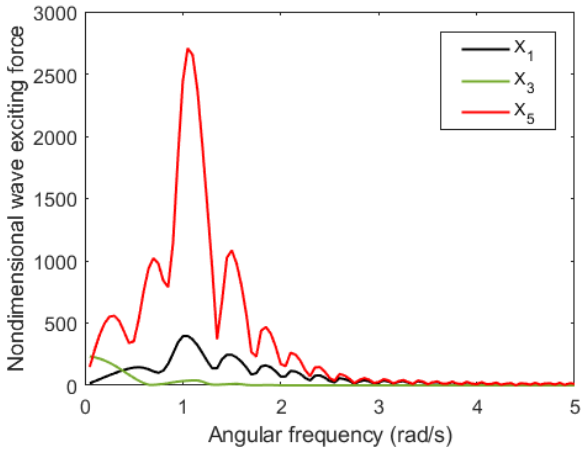

Fig. 7. Nondimensional wave exciting force of the platform calculated by WAMIT

3.1 Design evaluation

The coupled numerical model is established in FAST with all the properties determined. Free-decay tests, Campbell diagram analysis and RAO analysis are conducted to further evaluate the dynamic characteristics of the FOWT and the details are presented in this section.

The free-decay simulation was carried out by giving an initial displacement along a specific DOF of the platform and allowing the structure to oscillate freely and regain its initial state. The natural periods in 6 DOFs are obtained and summarized in Table 4, and, it is clear from the table that the natural periods of the present platform satisfy with the recommended value given by DNVGL-RP-0286 (DNVGL, 2019).

Table 4. Natural periods of the platform

Mode	Natural period (s)	DNV standard (s)
Surge/sway	18.62	15-60
Heave	1.54	1-2
Roll	2.23	2-5
Pitch	2.32	2-5
Yaw	14.71	8-20

To further evaluate the performance of the FOWT considering the entire system natural frequencies, the eigen analysis of the wind turbine is performed to obtain the first- and second-order frequencies of the tower and presented in the Campbell diagram (Fig.8). The Campbell diagram is widely utilized to describe the necessary damping during the operation of wind turbine and of great importance to interpret the dynamic responses of the full nonlinear system (Bonello, 2019). In the present study, Campbell diagram analysis is conducted to inspect if the natural frequencies of the redesigned platform interfere with the key frequencies of the tower vibration and the dynamic damping generated during the pass through of the rotor.

The red dash lines show the operational range (cut-in and cut-out rotor speeds 6.9 rpm and 12.1 rpm respectively) of NREL offshore 5-MW baseline wind turbine, while the black solid lines indicate the periodic aerodynamic loads excited by the rotor rotation. The overlap of the lines indicating different item of structure's dynamic damping exits within the range of operational rotor speed may raise risk of resonance of the structure. 1P and 3P frequencies are generated by the rotation of the rotor and each single blade respectively, which are the important parameters considered in the design of wind turbine. It is obvious from Fig. 8 that the platform's surge, sway, heave and yaw natural frequencies do not interact with any of the turbine periodical motions (i.e. 1P, 3P, 6P etc.), the tower first and second fore-aft (FA) and side-to-side (SS) frequencies and blade and drivetrain frequencies within the region between the lower and upper limits of the rotor speed. The lines representing pitch and roll natural frequencies overlap with the turbine 3P frequency, which indicate that the responses have the risk of resonance. In consideration of the low order of platform pitch and roll responses for TLPs, it is assumed that the effect of interaction is limited at the design stage. However, it is necessary to further investigate by sufficient dynamic response analysis, which is discussed in the next section.

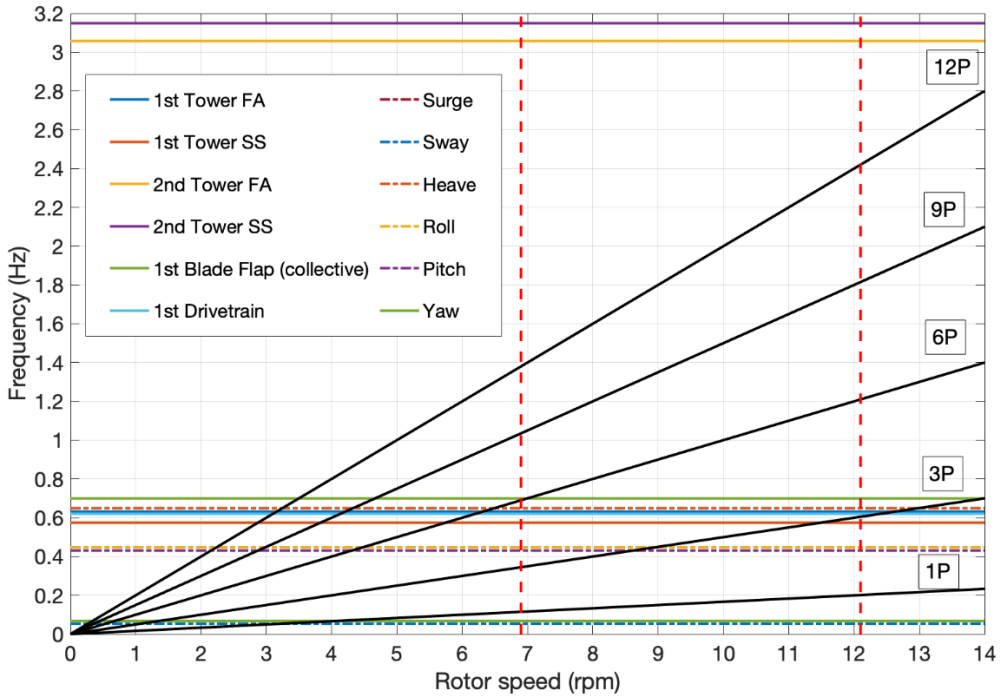

Fig. 8. Campbell diagram of TLP FOWT

The Response Amplitude Operators (RAOs) of the platform are computed using the method introduced in Ramachandran et al. (2013). The detailed calculation process is described as follow. The time-domain simulation is run in FAST with a rigid (resulting in only 6 platform DOFs) wind turbine. The aerodynamic load is calculated without wind inflow. The time-domain wave signal input to the HydroDyn module is described using a white-noise spectrum with a wave height of 2 m. The band width of input wave ranging from 0.1 rad/s to 6.28 rad/s to cover the eigen frequency of the platform in all DOFs. Three runs of simulations are carried out using different wave seeds, each with a time duration of 8000 s. The time-domain responses and wave time histories are performed by excluding the transients of the first 2000 s and the rest of data are transformed to frequency-domain spectrum using Fast Fourier Transform function in Matlab, and the RAOs in surge, heave, pitch and yaw are calculated based on the following equation:

$$RAO_i = \sqrt{\frac{S_i}{S_{Wave}}} \tag{3}$$

where, i is the mode associated with the platform DOF, S_i and S_{Wave} are the spectral response in i^{th} mode and wave respectively. For each DOF, the results were obtained by averaging the three computations. The RAOs are plotted in Fig.9 and it can be observed that the response of the platform is dominated by surge with the amplitude of 9.67 m/m at the surge natural frequency. The platform motions in heave, pitch and yaw are relatively small, illustrating the stability of the TLP platform in the corresponding directions. In addition, the responses in pitch is obviously coupled with surge.

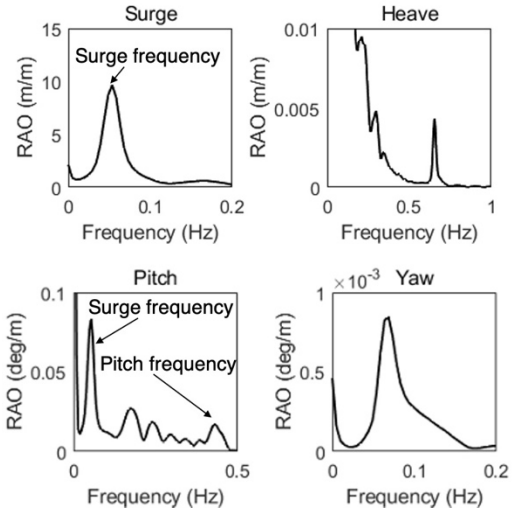

Fig. 9. RAOs of TLP platform in surge, heave, pitch and yaw

4. Dynamic response analysis of FOWT

4.1 Load cases

A set of joint wave and wind conditions are selected to examine the performance of the FOWT under real sea states. The stochastic wind simulator TurbSim is used to generate the 145 m x 145 m turbulent wind field based on the IEC Kaimal spectral model. The turbulence intensity corresponding to the wind speed was determined using IEC Class C turbulence model in the simulation. (J. Jonkman & M.L. Buhl, 2006). The wind shear exponent is selected to be 0.1, which is a typical value for offshore applications (Hsu et al., 1994). The wave condition is described by two associated parameters, significant wave height, H_S and spectral

peak period, Tp. The JONSWAP spectrum was used for simulating waves in this study, which is given by Equation (3) according to IEC 61400-3,

$$S(\omega) = \frac{1}{2\pi}\frac{5}{16}H_s^2 T_p \left(\frac{\omega T_p}{2\pi}\right)^{-5} exp\left[-\frac{5}{4}\left(\frac{\omega T_p}{2\pi}\right)^{-4}\right][1 - 0.287 \quad \ln(\gamma)]\gamma^{exp\left\{-0.5\left[\frac{\frac{\omega T_p}{2\pi}-1}{\sigma(\omega)}\right]^2\right\}} \qquad (4)$$

where γ is the peak enhancement parameter of a given irregular see state, and σ is a scaling factor. The wave spectrum is transformed to the time-domain by inverse Fast Fourier Transform (IFFT) function in HydroDyn and utilized for the calculation of wave kinematics.

For this study, six sets of environmental conditions are selected based on the target site sea state and the turbine properties. Environment conditions E1 and E2 are determined as two operational conditions with the rated and over-rated hub height wind speed, while E3 and E4 aim to test the FOWT under survival sea states. The incident wind and waves are collinear in E1 to E4, while an angle of 30° was set for E5 and E6 to examine the effect of wind-wave misalignment. The wind is always assumed to flow along the positive X direction while the misalignment is achieved by turning the propagating direction of waves to 30°. Based on the six environmental conditions, a total of 12 load cases are determined combining different tendon failure scenarios and turbine state. For each load case, the simulation lasts for 3 hours (10800 s) and the computations are repeated for three times using different seed number for wave generation. The results are analysed using time- and frequency-domain approaches. For the time domain analysis, an example of time-series result will be performed for each load case among the 3 repeated runs. For the frequency analysis, the PSD curves were calculated by averaging the runs with 3 different seeds, with exclusion of the results of the first 1800 s to avoid transient effect. The details of the load cases are summarized in Table 5.

The three different tendon states are 'Intact', 'T1 Broken' and 'T2 Broken', denoting the different failure scenarios. In the load cases that are labelled as 'T1 Broken', the tendon T1 (refer to Fig. 1), which is located at the upward column, was broken at 1050 s after the simulation has started. Same convention was used for another tendon, e.g. 'T2 Broken'. For LC

1 and LC 2, where the tendon remains intact under the operational environmental condition, the turbine rotates during the 3-hour simulation. For load cases that one tendon has failed when operational environmental conditions applied, the turbine was normally operating at the beginning of the simulation and then was shut down at the moment of tendon failure (1050 s). For load cases simulated with extreme environmental conditions E3, E4 and E6, the turbine remains parked regardless the tendon's state.

Table 5. Description of load cases

Load case	Environ-ment	H_S (m)	T_P (s)	V_{Hub} (m/s)	Wave direction	Tendon state	Rotor state
LC 1	E1	4.928	10	11.25	0	Intact	Rotate
LC 2	E2	5.4	7.5	25	0	Intact	Rotate
LC 3	E3	10	13.9	41	0	Intact	Park
LC 4	E4	7.6	13.2	41	0	Intact	Park
LC 5	E1	4.928	10	11.25	0	T1 Broken	Rotate-park
LC 6	E3	10	13.9	41	0	T1 Broken	Park
LC 7	E1	4.928	10	11.25	0	T2 Broken	Rotate-park
LC 8	E5	4.928	10	11.25	30	T1 Broken	Rotate-park
LC 9	E5	4.928	10	11.25	30	T2 Broken	Rotate-park
LC 10	E3	10	13.9	41	0	T2 Broken	Park
LC 11	E6	10	13.9	41	30	T1 Broken	Park
LC 12	E6	10	13.9	41	30	T2 Broken	Park

4.2 Dynamic response analysis of FOWT under intact conditions

The performance of the FOWT under operational and extreme sea states is examined by applying the above defined twelve load cases. Figs. 10-15 present the time series of wave elevation, surge, heave, pitch, line #4 tension and tower top acceleration, between 2000 s to 3000 s of the simulation, and the corresponding power spectral densities (PSDs) during the 3-h simulation for only LC 1 (operational condition) and LC 3 (extreme condition). As expected, higher responses are seen for LC3 than LC1 as the environment is harsher in LC 3. The surge

and pitch displacements, the mooring tension and the tower top acceleration for these two environments have peak values at the wave frequency in the spectral plots. The PSD of heave displacement (Fig. 12) shows two peaks, one at the wave frequency and second at twice the wave frequency. This is caused by surge and heave coupling, which is usually observed for TLPs with high tendon stiffness and shallow water depth, known as the set-down effect (Demirbilek, 1990) . The maximum, minimum, mean and standard deviation (STD) of the platform responses of LC 1 to LC 4 are summarized in Table 6. It is to be noted that the maximum mooring tension of T1 under intact condition, which also represents the highest tension force of 8976 kN among the 6 tendons, remains below the minimum breaking load of 20307 kN. The statistics of tendon failure cases are discussed in the next section.

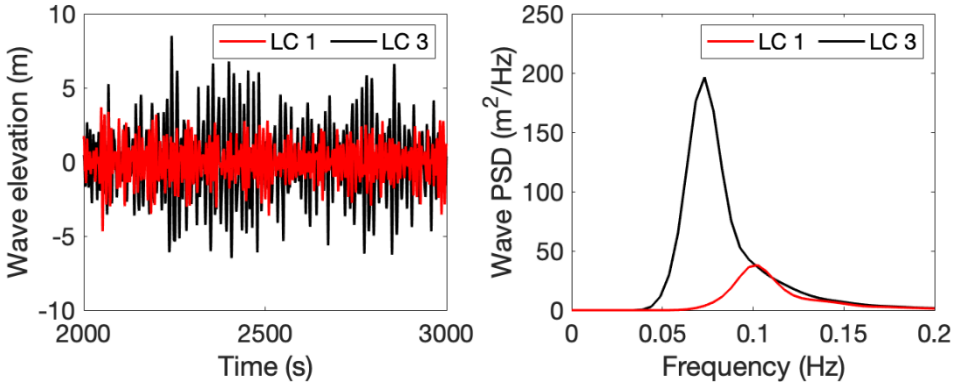

Fig. 10. Time series wave elevation and PSD at LC 1 and LC 3

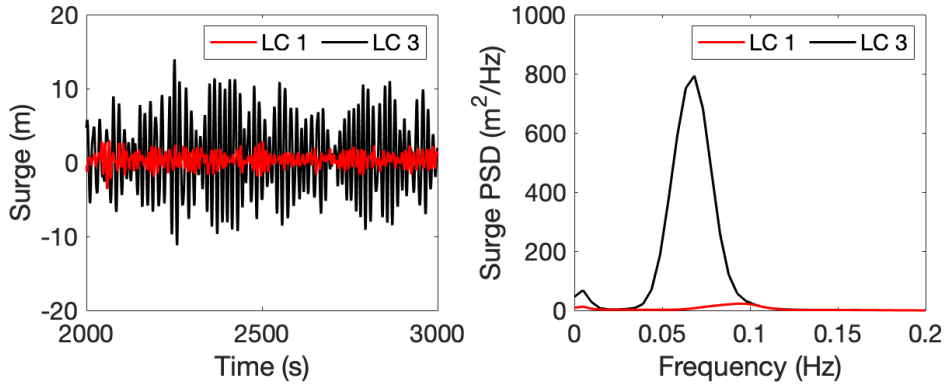

Fig. 11. Time series platform surge and PSD at LC 1 and LC 3

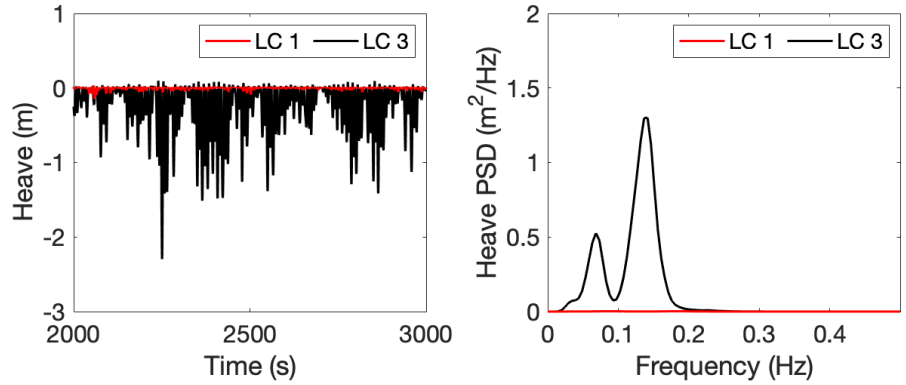

Fig. 12. Time series platform heave and PSD at LC 1 and LC 3

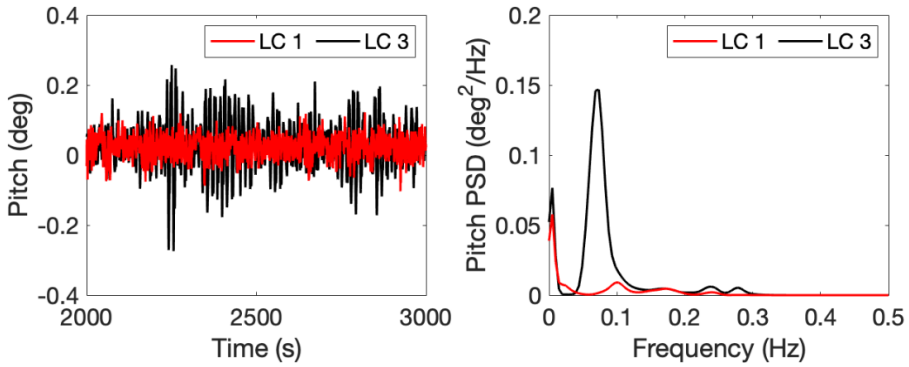

Fig. 13. Time series platform pitch and PSD at LC 1 and LC 3

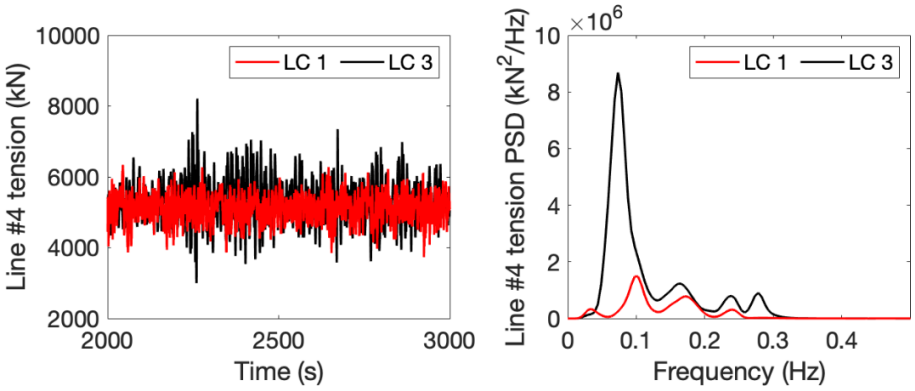

Fig. 14. Time series mooring tension of line #4 and PSD at LC 1 and LC 3

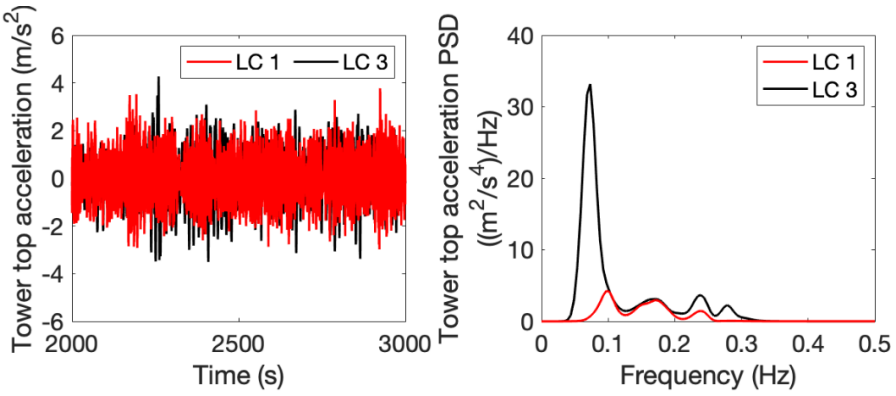

Fig. 15. Time series tower top acceleration and PSD at LC 1 and LC 3

Table 6. Statistics of platform responses

		LC 1	LC 2	LC 3	LC 4
Surge (m)	MAX	3.930	3.127	14.870	11.850
	MIN	-3.610	-4.389	-11.520	-9.433
	MEAN	0.356	0.423	0.804	0.694
	STD	0.985	0.594	4.642	3.366
Heave (m)	MAX	0.034	0.033	0.181	0.127
	MIN	-0.178	-0.217	-2.624	-1.649
	MEAN	-0.005	0.001	-0.241	-0.124
	STD	0.018	0.010	0.310	0.175
Pitch (deg)	MAX	0.132	0.213	0.393	0.263
	MIN	-0.104	-0.201	-0.389	-0.246
	MEAN	0.024	0.024	0.028	0.028
	STD	0.030	0.042	0.071	0.048
Yaw (deg)	MAX	0.332	0.669	0.247	0.198
	MIN	-0.429	-0.849	-0.203	-0.184
	MEAN	-0.038	-0.093	0.016	0.016
	STD	0.108	0.227	0.061	0.052
T1 tension (kN)	MAX	6473	7507	8976	7549
	MIN	3670	2635	1870	2983
	MEAN	5123	5128	5307	5249
	STD	365	510	653	468

4.3 Tendon failure analysis

The dynamic responses of the FOWT under tendon failure scenarios presented and discussed in this section. The effects of wind-wave misalignment were investigated, and the breakage occurs on the tendon attached on different columns was also considered.

According to the mooring failure analysis conducted for the catenary-moored semisubmersible FOWT (Bae et al., 2017), the most significant change to the platform after one mooring line has failed, is the long drift in the surge direction. However, the present study shows that for the TLP-type FOWT, the change of platform response in surge is limited. The

difference between the mean platform surge for the intact and failed conditions is less than 2%. This is because the horizontal movements of the TLP platform are not sensitive to the mooring stiffness and the position of the platform is restrained by the remaining tendon adjacent to the broken one. Therefore, the analysis in the present study is mainly focused on the change of response in platform pitch, heave and mooring tension

The response time series of platform in heave, pitch, roll and yaw, the tower top acceleration and the tension forces in T4 and T5 for LC 5 and LC 7, where tendons T1 and T2 are broken under the operational environmental condition E1 are shown in Fig. 16. The platform shows similar responses in heave and yaw when the tendon attached on different columns are broken (upward and leeward column). It can be seen that the platform heave increases up to 0.15 m at the moment of tendon broken. The averaged heave position increased from -0.005 m to 0.067 m after the failure. The platform yaw response (its magnitude was small though before the failure) and the tower top acceleration both decreased after the tendon breakage, this is mainly because the turbine was shut down, leading to lower perturbance led by the aerodynamic loadings. This suggests that a control strategy should be properly determined to avoid significant transient response when tendon failure occurs.

Different responses are observed in platform pitch and roll when the tendon attached on different column have failed. The mean pitch angle increases from 0.024° to 0.242° when T1 is broken and decreased to -0.124° when T2 was lost. In terms of platform roll, the average value remained the same after T1 was lost, while the amplitude got much smaller due to the halt of the turbine. In the case of T2 failure, both the amplitude and the mean value in platform roll motion increased significantly. The transient response reached 0.353°. Although the relative increase in the rotational movements seem remarkable, the highest value is below 1°, which can be seen to be less effective to the overall system. The change of tension force in the adjacent tendon is remarkable among the two failure scenarios. The maximum tension increased to 13070 kN in LC 5 and 12410 kN in LC 7, the safety factors are therefore calculated to be 1.55

and 1.64, respectively, which satisfy the recommended minimum value of 1.1 given in DNVGL-OS-E301 (DNV, 2015) for Accidental Limit State (ALS).

The results for LC 7 and LC 10, which depicts the tendon failure under the extreme environmental condition (E3) are shown in Fig. 17. A slight increase in heave after the loss of tendon under the extreme condition was observed, which is much less than the change seen under the operational condition. The platform's yaw motion and the tower top acceleration show larger amplitude after the tendon failure. The behavior in pitch and roll show similar trend with LC 5 and LC 7. The key observations from the above are that, (i) most of the platform motions and tendons forces are affected by the tendon failure, and, (ii) depending on the environments used for modelling, different responses are noticed, and these should be carefully taken into account when evaluating the design.

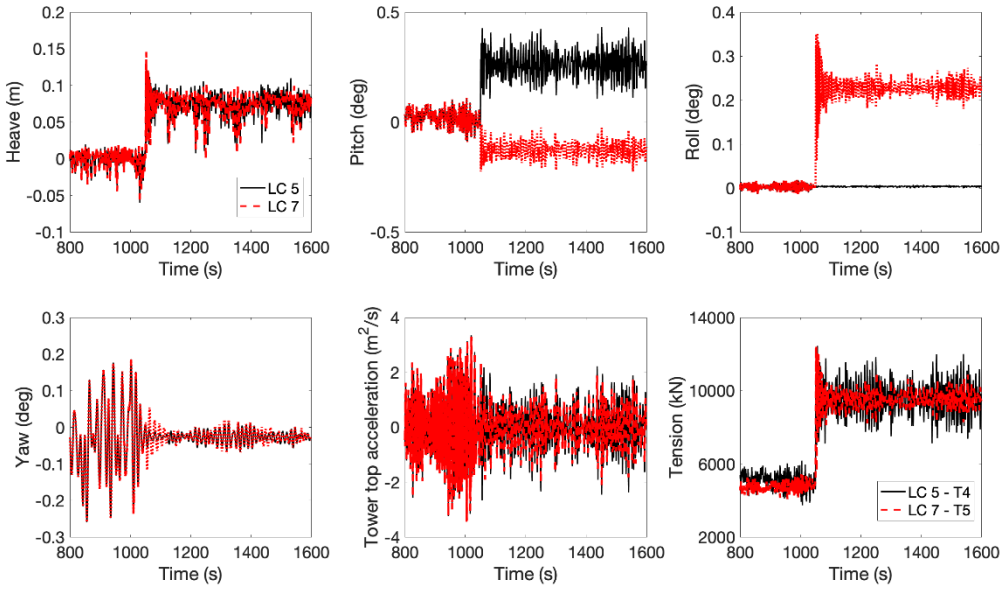

Fig. 16. Time series responses of FOWT for LC 5 and LC 7 (H_S = 4.928 m, T_P = 10 s, V = 11.25 m/s)

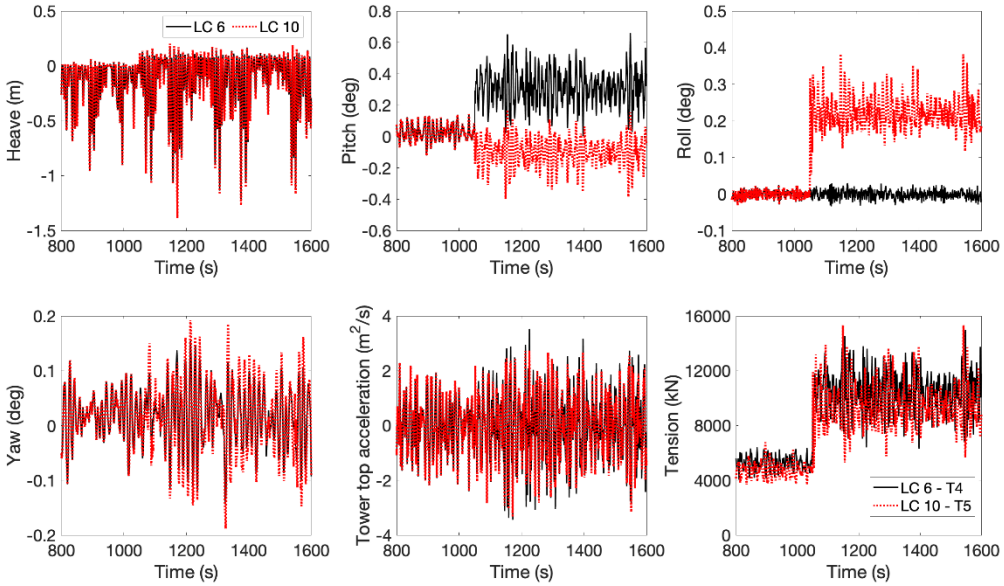

Fig. 17. Time series responses of FOWT for LC 6 and LC 10 (H_S = 10 m, T_P = 10.39 s, V = 41 m/s)

The misalignment between wind and waves also affect the responses of FOWT. Taking an extreme sea state as an example, the boxplot, presenting the mean, maximum, minimum, Q1 and Q3 for the results of LC 3, LC 6, LC19, LC 11 and LC 12 is given in Fig. 18. While the mean values of heave, yaw and tower top acceleration remain almost the same for all cases, pitch, roll, T4 and T5 tensions are varying with load cases. The maximum roll motion under the misalignment scenario is about 23 times than that of the collinear scenario when T1 was lost, and, about 2.5 times when T2 was lost. Hence, the effect of misalignment on platform roll is more predominate after T1 has failed. The maximum yaw response raised from 0.249° in LC 6 to 4.957° in LC 11 and from 0.293° in LC 10 to 4.925° in LC 12, indicating that the angle between wind and waves leads to significant response. The tower acceleration remained at the same level for all the five load cases since it is mainly affected by the aerodynamic loading

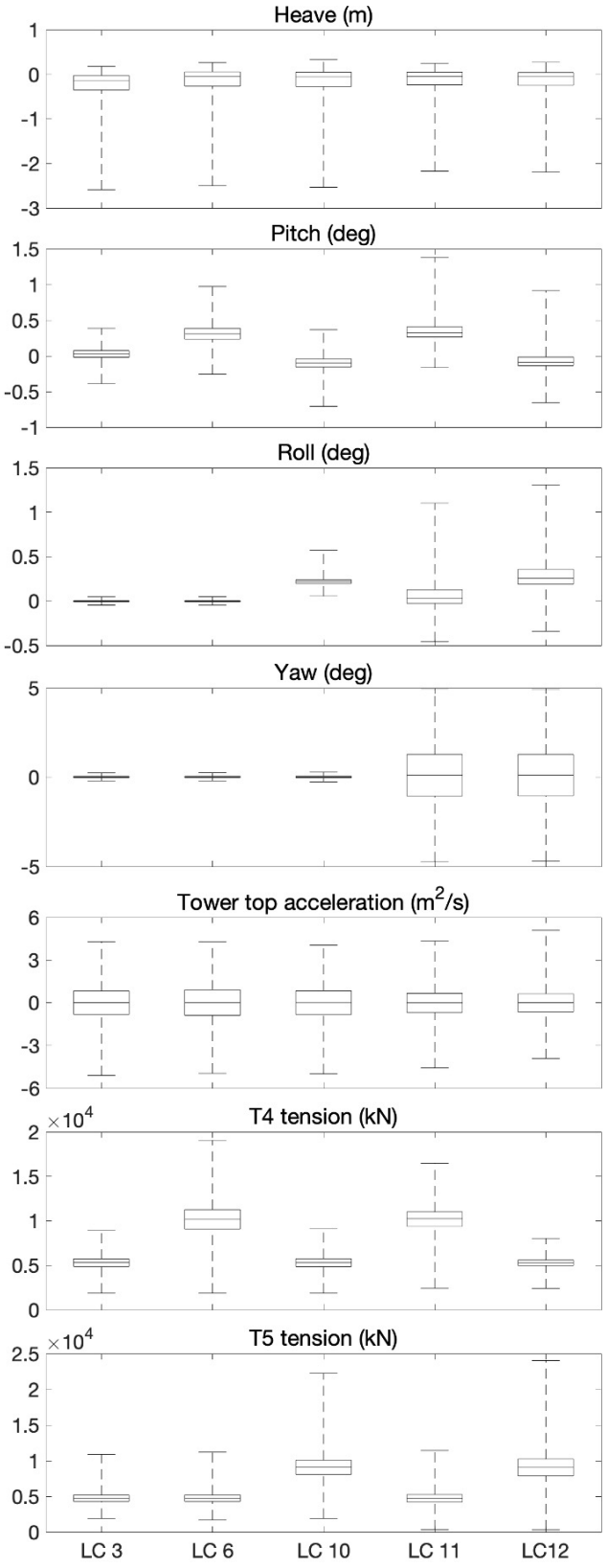

Fig.18. Statistics of FOWT responses for different load cases

In order to further understand the different responses with time, a wavelet transform analysis was carried out. This is an approach of localized time-frequency analysis which

applies when signals have short intervals of characteristic oscillation and short signal pieces have significance. Under the tendon failure scenarios, it is insufficient to interpret the change of frequency-domain response that persist over an entire signal and ignore the transient effect that may deliver significant information by the data analysis (Talebi, 2020). The outcomes of the wavelet transform analysis are presented in Figs. 19-21. Fig.19 depicts the behavior of heave response and the peak responses are seen to be concentrated around two frequencies, one around 0.75 Hz and another around 1.5 Hz, which agrees well with the heave spectra shown in Fig 12. Nevertheless, the heave motion does not seem to be significantly affected by tendon failure, as no obvious change to wavelets are seen after 1000 s when the tendon failure was initiated. However, a clear change is seen in the pitch response in Fig.18, where in addition to the primary peak at 0.072 Hz, a shift in frequency to 0.25 Hz occurs after 1000 s. The similar activity can also be observed in the mooring line force of line T4 (see Fig.20). In addition, the energy content of mooring tension increases at the wave frequency after the tendon fails.

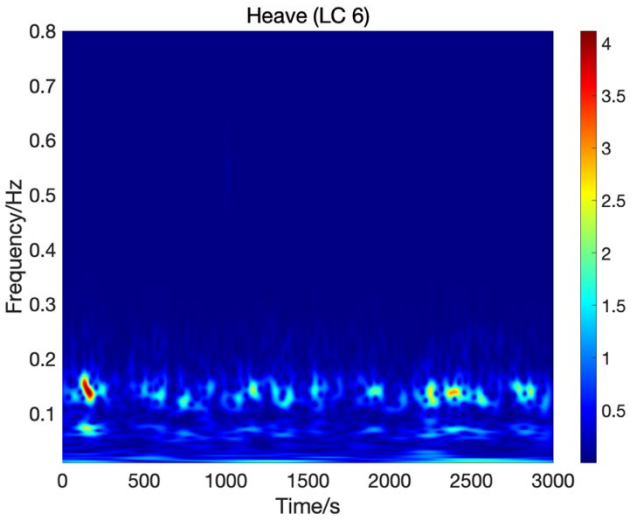

Fig. 19. Wavelet transformation of platform heave at LC 6

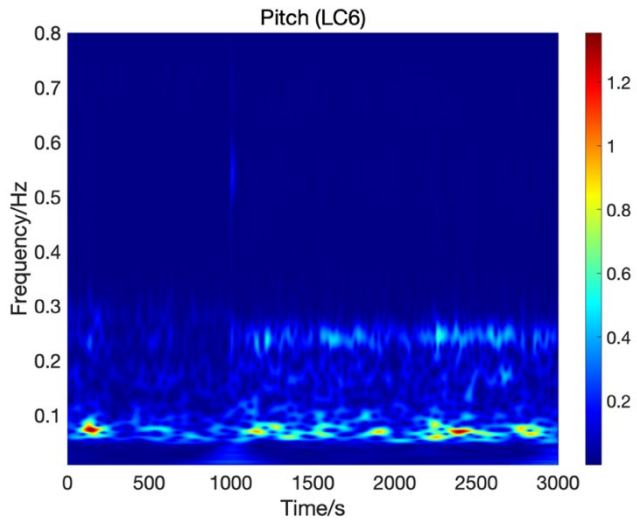

Fig. 20. Wavelet transformation of platform pitch at LC 6

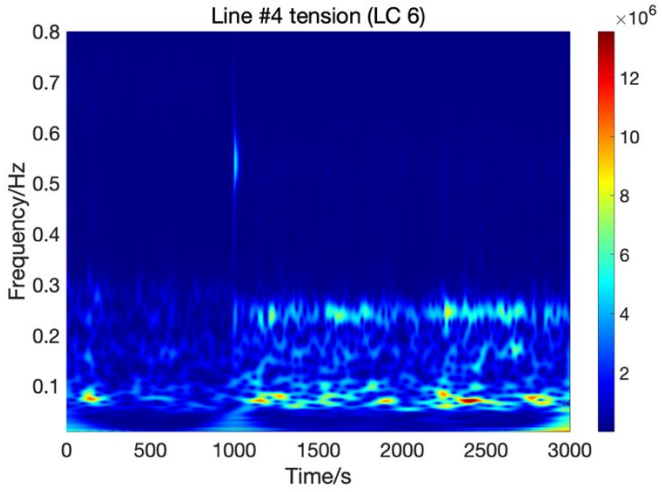

Fig. 21. Wavelet transformation of T4 tension at LC 6

Due to the complex nature of modelling of FOWT dynamics, there may be uncertainties involved in quantifying the response. The uncertainties of the analysis mainly come from the assumptions used in building the simulation model with the platform interacting with different environments. For example, the platform is assumed as a rigid body without considering hydroelasticity and the resulting deformation, which may alter the characteristics of the structure. The turbulence intensity can be different across the rotor area and this would lead to different aerodynamic loading. The waves considered here are linear waves generated using JONSWAP spectrum, however, it is possible that the responses could have been nonlinear, but difficult to quantify its contribution. Tendons response was assumed to be

linear after the failure which might not be true. Therefore, this work merits further study in the future to provide more insight for improving the research, design and operation. One possibility is to validate the results with physical model experiments, and this has been underway, and the results will be reported in the near future. The progressive optimization of the structure design and control strategy determination can be also conducted based on the tendon failure analysis.

5. Conclusion

The dynamic response of a 5-MW TLP type floating offshore wind turbine platform with its tendon failure was simulated using the NREL FAST numerical tool. The hydrodynamic performance was evaluated by employing WAMIT and ANSYS/AQWA software tools. The non-dimensional added mass, damping coefficients and first-order wave exciting forces computed using these two tools have been compared and discussed. The results showed good agreement, and thus helped to verify the reliability of the hydrodynamic calculations.

The natural frequencies of the FOWT in 6 DOFs, the Campbell diagram and the response amplitude operators (RAOs) have been analyzed to evaluate the performance of the system designed. Twelve load cases, representing the operational and survival environmental conditions and the tendon failure scenarios, were selected for the dynamic analysis. The simulated time series of platform responses, tension forces and the tower top acceleration corresponding to these twelve load cases were presented.

1. The proposed design of the TLP FOWT was found to be highly stable as indicated by the limited heave and pitch RAOs. The natural frequencies of the platform agreed with the recommendations given in the DNV design standard. The platform's surge, sway,

heave and yaw natural frequencies are out of the range of turbine's periodic effect, while pitch and roll responses have the risk of interaction with 3P response.

2. The results of dynamic analysis showed significant response of the FOWT under survival conditions in surge.
3. The spectral analysis of the platform's heave response was observed to have two peaks, one at the wave frequency and other at twice the wave frequency, and the latter was associated with coupled heave and surge motion.
4. The effect of tendon failure was reflected in the change of frequency shifting of the platform's pitch and the tension in the non-broken tendons. The maximum pitch angle after tendon failure occurred was 0.973° for the most extreme sea state, which is more than three times than that of the intact state.
5. The average and dynamic safety factor of the tendon experiencing the highest tension was 2.04 and 1.11 respectively, both satisfied the recommended values specified in design standard.
6. The loss of tether T1 led to the increase of platform's pitch along the wave direction (noted as positive amplitudes), while tether T2 failure resulted in larger negative pitch. However, the values of pitch and roll magnitudes were fairly small, i.e. less than 1^{o}.
7. Misalignment between wind and waves led to significant increase in platform's roll and yaw. The largest yaw angle reached 4.957° for the case of tether T1 broken.
8. From the wavelet transform analysis, it was found that, the energy content of the platform's pitch and tension for tether T4, increased at shifted pitch frequency and wave frequency, indicating that the platform response to wave became stronger with

the damaged tendon system.

In summary, this work has demonstrated how the FOWT performance was affected by failure of a mooring line purely by numerical methods and therefore care should be exercised when applying the results to practical design, as the results have not been verified by other means, for example, a model scale testing.

Acknowledgement

This research work was supported by the Institute for Energy Systems, School of Engineering at the University of Edinburgh, United Kingdom. The first author is grateful to the Royal Society of Edinburgh, for the funding provided through the John Moyes Lessells Travel Scholarship to undertake research at Dalian University of Technology, China. Also, the third author acknowledges the funding received from the National Natural Science Foundation of China (Grant No. 52071058 and No. 51939002). This work is also partially supported by LiaoNing Revitalization Talents Program (XLYC1807208) and the Fundamental Research Funds for the Central University (DUT20ZD219).

References

Vryhof Anchors, 2021. Anchor Manual 2010: The Guide to Anchoring.

ANSYS Inc., 2017. ANSYS AQWA, Librium. NAUT and Tether Manuals.

Bae, Y. H., Kim, M. H., & Kim, H. C., 2017. Performance changes of a floating offshore wind turbine with broken mooring line. *Renewable Energy, 101*, 364-375. doi:https://doi.org/10.1016/j.renene.2016.08.044

Bonello, P., 2019. The extraction of Campbell diagrams from the dynamical system representation of a foil-air bearing rotor model. *Mechanical Systems and SIgnal Processing, 129*, 502-530.

Crozier, A., 2011. *Design and Dynamic Modeling of the Support Structure for a 10 MW Offshore Wind Turbine.* Master's Thesis. NTNU.

Cruz, A., Krausmann, E., 2008. Damage to Offshore Oil and Gas Facilities Following Hurricanes Katrina and Rita: An Overview. *Journal of Loss Prevention in The Process Industries, 21*, 620-626.

Demirbilek, Z., 1990. Design formulae for offset, set down and tether loads of a tension leg platform (TLP). *Ocean Engineering, 17*(5), 517-523. doi:https://doi.org/10.1016/0029-8018(90)90042-5

Ding, H., Han, Y., Zhang, P., Le, C., Liu, J., 2016. Dynamic Analysis of a New Type of Floating Platform for Offshore Wind Turbine. *Proceedings of the Twenty-sixth International Ocean and Polar Engineering Conference, Rhodes, Greece.*

DNV GL, 2015. DNVGL-OS-E301 Position mooring.

DNV GL, 2019. DNVGL-RP-0286 Coupled analysis of floating wind turbines.

DNV GL, 2018. DNVGL-ST-0119 Floating wind turbine structures.

EDP, 2021. Floating offshore wind-power generating platform. URL: https://www.edp.com/en/innovation/ windfloat

Equinor, 2021. Hywind Scotland remains the UK's best performing offshore wind farm. URL: https://www.equinor.com/en/news/20210323-hywind-scotland-uk-best-performing-offshore-wind-farm.html

GustoMSC, 2021. Floating Wind Tri-Floater. URL: https://www.gustomsc.com/design/floating-wind/tri-floater

GWEC, 2020. Global Offshore Wind Report 2020.

Hsu, S. A., Meindl, E. A., Gilhousen, D. B., 1994. Determining the Power-Low Wind-Profile Exponent under Near-Neutral Stability Conditions at Sea. *Journal of Applied Meteorology and Climatology, 33*(6).

Ideol, B., 2021. FRANCE'S FIRST OFFSHORE WIND TURBINE AND BW IDEOL'S FIRST DEMONSTRATOR FLOATGEN. URL: www.bw-ideol.com/en/floatgen-demonstrator

Jonkman, J., 2010. Definition of the Floating System for Phase IV of OC3 (NREL/TP-500-47535).

Jonkman, J., M.L. Buhl, J., 2006. TurbSim User's Guide (NREL/TP-500-39797).

Jonkman, J. M., 2009. Dynamics of Offshore Floating Wind Turbines—Model Development and Verification. *Wind Energy, 12*, 459-492. doi:10.1002/we.347

Jonkman, J. M., Jr., M. L. B., 2005. FAST User's Guide.

Lefebvre, S., Collu, M., 2012. Preliminary design of a floating support structure for a 5MW offshore wind turbine. *Ocean Engineering, 40*, 15-26.

Liu, J., Thomas, E., Manuel, L., Griffith, D. T., Ruehl, K. M., Barone, M., 2018. Integrated System Design for a Large Wind Turbine Supported on a Moored Semi-Submersible Platform. *Journal of Marine Science and Engineering, 6*(1), 9.

Mansour, A. M., Gordon, B. J., Ling, Q., Shen, Q., 2013. TLP Survivability Against Progressive Failure of Tendon and Foundation Systems in Offshore Western Australian Harsh Environment. P*roceedings of the ASME 32nd International Conference on Ocean, Offshore and Arctic Engineering, Nantes, France.*

Masciola, M., Jonkman, J., Robertson, A., 2013. Implementation of a Multisegmented, Quasi-Static Cable Model. *Proceedings of the International Ocean (Offshore) and Polar Engineering Conference, Anchorage, Alaska.*

Matha, D., 2009. Model development and loads analysis of an offshore wind turbine on a Tnesion Leg Platform, with a comparison to other floating turbine concepts. PhD Thesis. MIT.

Myhr, A., 2016. Developing offshore floating wind turbines: the Tension-Leg-Buoy design. PhD Thesis. NTNU.

Qi, Y., Tian, X., Guo, X., Lu, H., Liu, L., 2019. The Hydrodynamic Performance of a Tension Leg Platform with one-dendon failure. *Ships and Offshore Structures, 14*(5), 523-533. doi:https://doi.org/10.1080/17445302.2018.1518188

Ramachandran, G. K. V., Robertson, A., Jonkman, J. M., Masciola, M. D., 2013. Investigation of

Response Amplitude Operators for Floating Offshore Wind Turbines. *Proceedings of the 23rd International Ocean, Offshore and Polar Engineering Conference, Anchorage, Alaska.*

Talebi, S., 2020. The Wavelet Transform. URL: https://towardsdatascience.com/the-wavelet-transform-e9cfa85d7b34

Vijay, K. G., Karmakar, D., Soares, C. G., 2018. Long term response analysis of TLP-type offshore wind turbine. *ISH Journal of Hydraulic Engineering, 26*(1), 31-43. doi:10.1080/09715010.2018.1437790

Lee, C., Newman, J., 2019. WAMIT User Manual.

Whitfield, S., 2019. Lessons Learned From the Big Foot Mooring Incident. URL: https://jpt.spe.org/lessons-learned-big-foot-mooring-incident

Withee, J. E., 2004. *Fully coupled dynamic analysis of a Floating Wind Turbine System.* PhD Thesis. MIT

Wu, H., Zhao Y., He, Y., Shao, Y., Mao, W., Han, Z., Jiang, Z., 2021. Transient response of a TLP-type floating offshore wind turbine under tendon failure conditions. *Ocean Engineering, 220*(108486). doi:https://doi.org/10.1016/j.oceaneng.2020.108486

Yang, C. K., Kim, M. H., 2010. Transient Effects of Tendon Disconnection of a TLP by Hull-tendon-riser Coupled Dynamic Analysis. *Ocean Engineering, 37*(8-9), 667-677. doi:http://doi.org/10.1016/j.oceaneng.2010.01.005

Yang, C. K., Padmanabhan, B., Murray, J., Kim, M. H., 2008. The Transient Effect of Tendon Disconnection on the Global Motion of ETLP. *Proceedings of the 27th International Conference on Offshore Mechanics and Arctic Engineering, Estoril, Portugal.*

Zeng, X., Shi, W., Michailides, C., Zhang, S., Li, X., 2021. Numerical and experimental investigation of breaking wave forces on a monopile-type offshore wind turbine. *Renewable Energy, 175*, 501-509.

Zhao, Y., Yang, J., He, Y., 2012. Preliminary Design of a Multi-Column TLP Foundation for a 5-MW Offshore Wind Turbine. *Energies, 5*, 3874-3891. doi:10.3390/en5103874

Zhao, Z., Shi, W., Wang, W., Qi, S., Li, X., 2021. Dynamic analysis of a novel semi-submersible platform for a 10 MW wind turbine in intermediate water depth. *Ocean Engineering, 237*.